Chemistry International 6(3) (2020) 110-121

International Scientific Organization
http://iscientific.org/
Chemistry International
www.bosaljournals.com/chemint/

Corrosion inhibition of API 5L X80 pipeline steel in acidic environment using aqueous extract of *Thevetia peruviana*

Akens Hamilton-Amachree and Nkem Bartholomew Iroha*

Department of Chemistry, Federal University, Otuoke, P.M.B. 126 Yenagoa, Bayelsa State, Nigeria
*Corresponding author's E. mail: irohanb@fuotuoke.edu.ng.com, nkemib@yahoo.com

A R T I C L E I N F O

Article type:
Research article
Article history:
Received June 2019
Accepted September 2019
July 2020 Issue
Keywords:
Thevetia peruviana
Corrosion inhibitor
Acidic environment
X80 pipeline steel
Surface analaysis
Chemisorption
Freundlich isotherm

A B S T R A C T

Aqueous extract of *Thevetia peruviana* leaves were investigated as corrosion inhibitor for API 5L X80 pipeline steel in 1*M* H_2SO_4 solution using electrochemical and gravimetric techniques. The results reveal that *T. peruviana* inhibited the X80 pipeline steel corrosion in the acid medium in a concentration dependent manner. Potentiodynamic polarization results showed *T. peruviana* to be a mixed type inhibitor in 1*M* H_2SO_4 environment, whereas the impedance results revealed adsorption of the inhibitor species on the steel surface. The gravimetric results reveal that the adsorption mechanism of the inhibitor on the steel surface was chemisorption. The adsorption was in accordance with Freundlich adsorption isotherm and negative standard adsorption energy (ΔG^{o}_{ads}) obtained inferred that the adsorption was spontaneous and the interaction between the inhibitive molecules was found to be repulsive. Scanning electron microscopy (SEM) confirmed the formation of adsorbed film on the X80 pipeline steel surface. Results revealed that *T. peruviana* has potential to inhibit the correction and could possibly be used for corrosion inhibition in the acidic environment of steel.

Capsule Summary: The inhibitive effect of *T. peruviana* extract on the corrosion of X80 steel in 1*M* H_2SO_4 was studied using different techniques. The extract proved to be an efficient inhibitor with inhibition efficiency increased as a function of extract concentration.

Cite This Article As: A. Hamilton-Amachree and N. B. Iroha. Corrosion inhibition of API 5L X80 pipeline steel in acidic environment using aqueous extract of *Thevetia peruviana*. Chemistry International 6(3) (2020) 110-121. https://doi.org/10.5281/zenodo.3516565

INTRODUCTION

Corrosion of metals is a constant and continuous problem, often difficult to eliminate completely. It would be more practical and achievable to prevent corrosion than complete elimination. The corrosion of metals though unavoidable, is controllable. API 5L X80 steel is often used as piping material in the oil and gas industries. The steel is preferred in pipelines because of its excellent mechanical properties such as good fatigue resistance, high strength, good toughness and good corrosion resistance (Zhao et al., 2012; Wang et al., 2011). Acids are used in industries for cleaning, descaling and pickling of metallic structures, which dissolve the metal (Iroha and Chidiebere, 2017; Keles et al., 2008; Nwosu et al., 2013). Tetraoxosulphate VI acid is one of the chemicals most widely used for the removal of undesirable scale and rust in many industrial processes. The use of corrosion inhibitor is one of the most important methods of protecting steel corrosion in acidic media. The addition of corrosion inhibitors effectively protects the metal against an acid attack (Pradipta et al., 2019; Qasim et al., 2019; Tang, 2019).

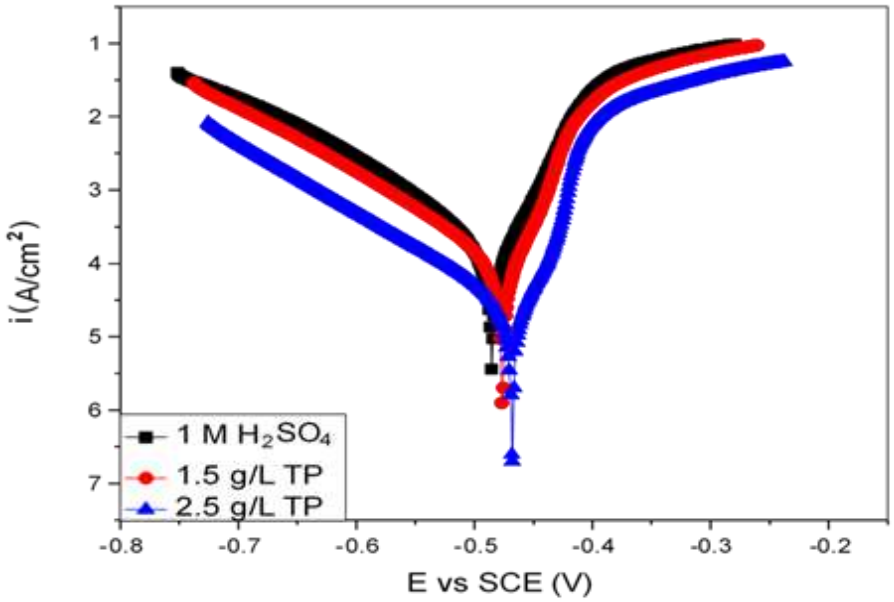

Fig. 1: PDP curves for the corrosion of X80 pipeline steel in 1 *M* H_2SO_4 without and with selected concentrations of *Thevetia peruviana* extract at 303 K.

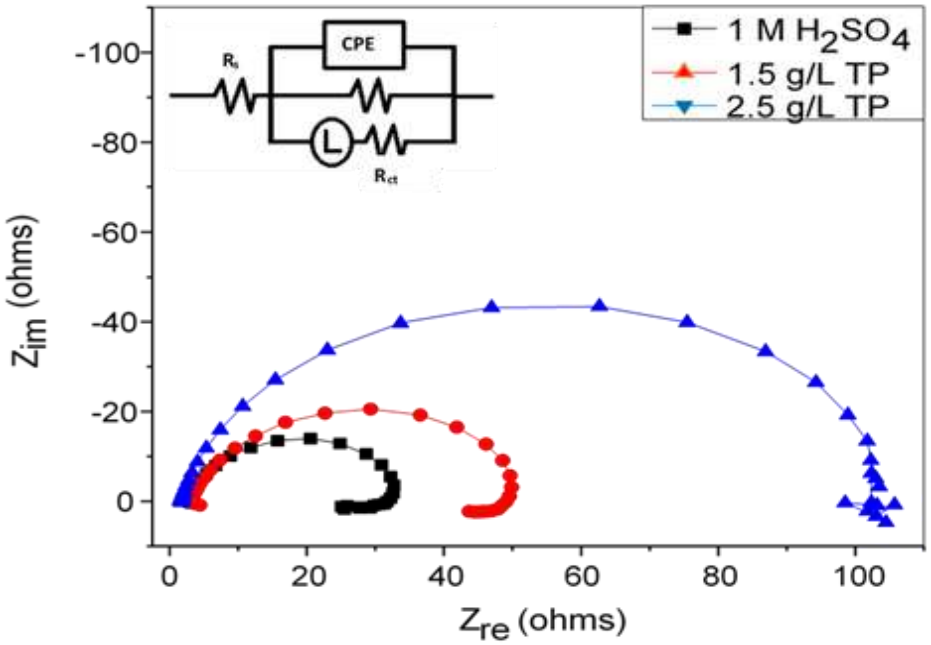

Fig. 2: Impedance plots for API 5L X80 pipeline steel in 1 *M* H_2SO_4 without and with selected concentrations of *Thevetia peruviana* extract at 303 K

The inhibition of metal corrosion is a surface process which involves the adsorption of the inhibitor on the metal surface. The use of natural products of plant origin as corrosion inhibitors is becoming the subject of extensive investigation (Iroha et al., 2012b; Ekanem et al., 2010; Nnanna et al., 2010; Loto et al., 2011; Soltani and Khayatkashani, 2015), probably due to the fact that these products are eco-friendly and readily available when compared with the synthetic and expensive hazardous inorganic and some organic inhibitors. The corrosion inhibition efficacy of these plant extracts is normally ascribed to the presence, in their composition, of complex organic species such as tannins, alkaloids, essential oils, pectin, anthraquinones, flavonoids and other nitrogen containing compounds (Belwal et al., 2018; Thakur et al., 2019).

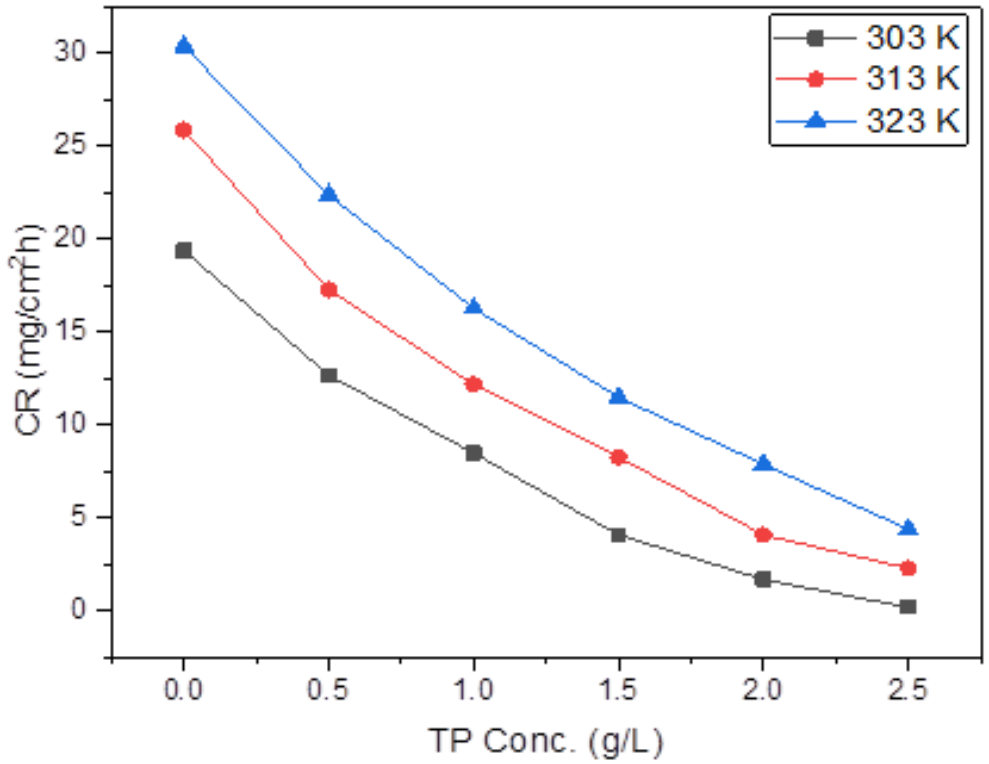

Fig. 3: Plot of corrosion rate against TP concentration in 1 *M* H_2SO_4 for X80 steel at different temperatures from weight loss measurements.

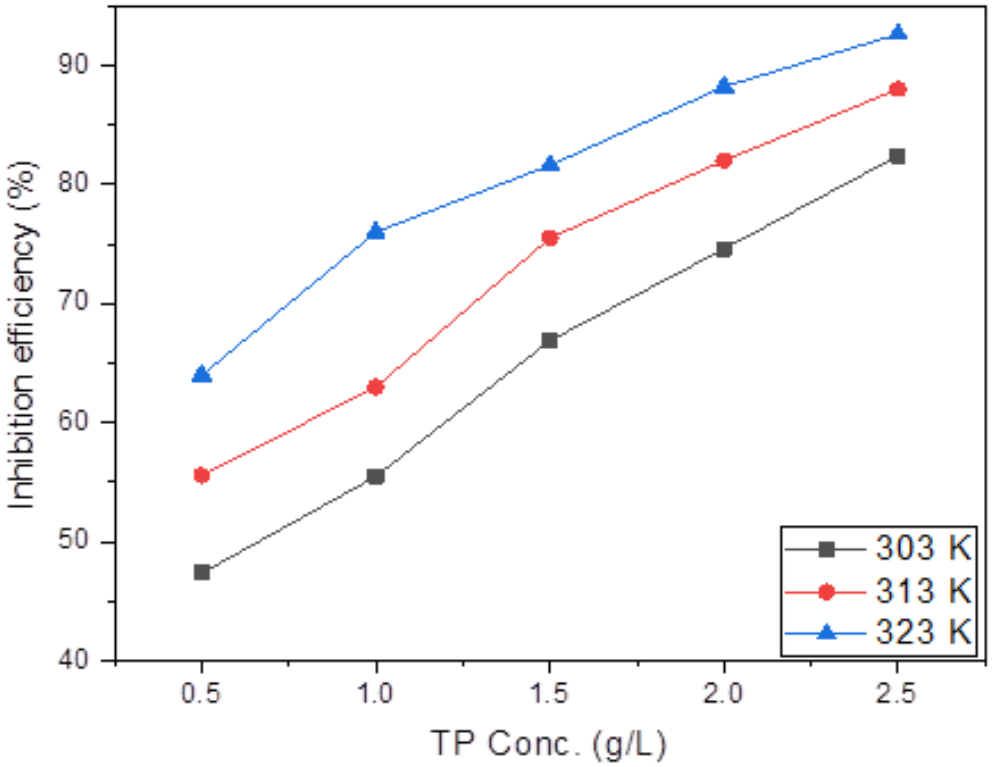

Fig. 4: Plot of inhibition efficiency against TP concentration in 1 *M* H_2SO_4 for X80 steel at different temperatures from weight loss measurements.

The plant material used for the present study, *Thevetia peruviana* (TP) commonly called yellow oleander is a small ornamental tree with leaves that are linear and spirally arranged (Samal et al., 1992). It is used medicinally to some extent, though it is also known to be very poisonous. All parts of the plants are very poisonous, especially the sap and oily seeds. The common name be-still refers to its poisonous properties. All parts of the plant contain a variety of cardiac glycosides which is believed to be responsible for its inhibitory action. This study sets out to investigate the role of aqueous extract of TP in monitoring the corrosion inhibition of API 5L X80 pipeline steel in 1*M* H_2SO_4 solution using potentiodynamic polarization (PDP), electrochemical impedance spectroscopy (EIS) and gravimetric techniques. Surface analyses were performed on the corroded surface using scanning electronic microscopy (SEM).

MATERIAL AND METHODS

Material preparation

X80 steel used for this study has the following chemical composition (weight %): C-0.065%, Si-0.24%, Mn-1.58%, P-0.011%, S-0.003%, Cu-0.01%, Cr-0.022%, Nb-0.057%, V-0.005%, Ti-0.024%, B-0.0006% and the balance is Fe. The API 5L X80 steel sheet was obtained from Shell Nigeria oil field. The X80 steel were cut into square shape samples with dimension 1.0 cm x 1.0 cm x 0.2 cm for surface analysis study and 2.0 cm x 2.0 cm x 0.2 cm for both gravimetric and electrochemical measurements. Prior to different experiments, each specimen was polished with emery papers, washed and degreased in acetone, dried and weighed. The blank acid (0.5 M H_2SO_4) was prepared by diluting Analar grade of the test acid in distil water.

T. peruviana (TP) leaves were procured from the herbarium of the Department of Botany, University of Port Harcourt, dried and ground to powder. A 10 g of the dried powder was boiled for 5 h in 1*M* H_2SO_4 solution. The resultant solution was cooled, filtered and then stored. From the stock solution of the plant extract, test solutions were prepared of 0.5, 1.0, 1.5, 2.0 and 2.5 g/L concentrations.

Electrochemical techniques

Electrochemical impedance spectroscopy (EIS) and potentiodynamic polarization (PDP) studies were conducted using the electrochemical workstation model CHI 660A and the E-chem analyst software was used to analyse the experimental data. The electrochemical measurements were carried out in a conventional three-electrode glass cell which consists of the X80 steel as the working electrode, a graphite rod as the counter electrode and a saturated calomel electrode (SCE) as reference electrode. The working electrode was encapsulated in epoxy resin of polytetrafluoroethylene (PTFE) leaving only flat surface of area 1 cm^2 exposed to the electrolyte. The exposed area was cleaned as earlier described. A steady state open circuit potential (OCP) was established for PDP and EIS experiments by immersing the X80 steel samples in the blank solution for 1 h. PDP measurements were carried out in the potential range from -250 mV to +250 mV relative to the corrosion potential using a scan rate of 1 mVs^{-1}. EIS measurements were performed at corrosion potential (E_{corr}) using a signal amplitude of 5 mV over a frequency range of 100 kHz to 10 mHz. Each experiment was conducted at 303 K and in quadruplicate to check the reproducibility.

Gravimetric measurements

Each X80 steel specimen previously weighed and recorded, was immersed into 100 mL of 1 M H_2SO_4 in the absence and presence of various concentrations of *Thevetia peruviana* (TP) leaves extract for an exposure time of 6 h at 303 K, 313 K and 323 K. After immersion, the square shaped samples were retrieved from the test solutions, washed with distilled water, degreased with ethanol, dried with acetone and accurately weighed, to determine the weight loss, which is taken as the difference in the weight of the X80 steel samples before and after immersion in different test solutions (Iroha et al., 2012a). Triplicate tests were run in each case and the mean value of the weight loss was reported. The corrosion rate (CR) (mg/cm^2h) in absence and presence of inhibitors, inhibition efficiency (%I_{WL}) in terms of weight loss measurements of the inhibitors and degree of surface coverage (θ) were calculated using Eqs. 1-3, respectively.

$$CR = \frac{\Delta W}{S.t} \quad (1)$$

$$\%I_{WL} = \left(\frac{CR_u - CR_i}{CR_u}\right)100 \quad (2)$$

$$\theta = \frac{\%I_{WL}}{100} \quad (3)$$

Where, ΔW is the weight loss, CR_u and CR_i are the corrosion rates of the X80 steel specimen without and with TP extract inhibitor respectively, S is the cross sectional area and t is the exposure time.

Surface analysis

Surface analysis of the X80 steel specimens in the absence and presence of the optimum concentration of TP at 303 K was examined using XL-30FEG Scanning electron microscope (SEM). The X80 steel specimens prepared as previously described in the gravimetric section were immersed for 6 h in 1 M H_2SO_4 solutions without and with 2.5 g/L *Thevetia peruviana* (TP) extract. The specimens were retrieved from the test solutions, cleaned in distilled water, dried in acetone and examined with SEM machine.

RESULTS AND DISCUSSION

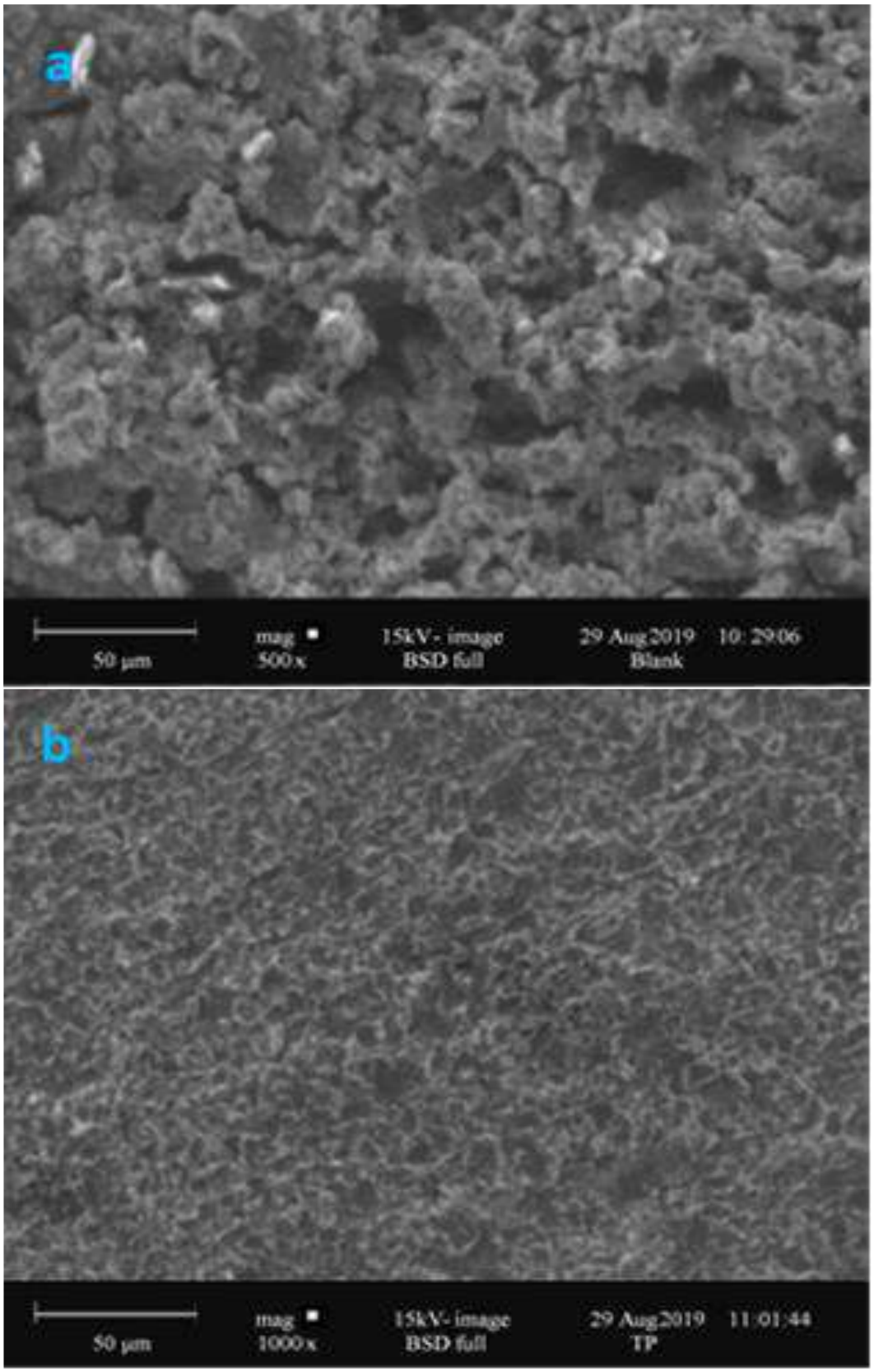

Fig. 5: SEM micrographs of X80 pipeline steel in (a) 1 *M* H_2SO_4 solution without TP extract (b) 1 M H_2SO_4 solution with optimum concentration of TP extract.

Potentiodynamic polarization (PDP) studies

Figure 1 depicts with an illustration the polarization curves of X80 steel in 1 M H_2SO_4 solution without and with selected concentrations of *Thevetia peruviana* (TP) extract at 303 K. The figure clearly shows that the addition inhibitor of TP reduces both cathodic and anodic metal reactions shifting their branches to the lower values of corrosion current densities and thus causing a remarkable decrease in the corrosion rate (Solmaz, 2010). This behaviour reflects the inhibitive tendency of TP extract. The electrochemical parameters, such as corrosion potential (E_{corr}), current density (i_{corr}), cathodic and anodic Tafel slopes (β_c and β_a), derived from the polarization curves in Figure 1 are listed in Table 1. The data shows that the corrosion current density (i_{corr}) is significantly decreased upon addition of the TP extract which indicates that the inhibitor molecules are adsorbed on the steel surface thereby blocking the corrosion active sites. The corrosion potential (E_{corr}) show a shift towards more positive potential with increase in TP concentration. However, the maximum displacement in E_{corr} was evaluated as 31.4 mV vs. SCE which categorizes TP as a mixed type inhibitor as the value is less than ±85 mV vs. SCE (Wang, 2011; Iroha and Nnanna, 2019). Table 1 also shows that the Tafel slopes, β_a and β_c at 303 K reduced upon addition of the inhibitor supporting the statement that TP extract is a mixed-type inhibitor. The percentage inhibition efficiency ($\%IE_{PDP}$) was calculated from i_{corr} values using Eq. 4.

$$\%IE_{PDP} = \left[\frac{i^{u}_{corr} - i^{i}_{corr}}{i^{u}_{corr}}\right]100 \quad (4)$$

Where, i^{u}_{corr} and i^{i}_{corr} are the corrosion current densities in blank acid and in presence of inhibitor, respectively. The values $\%IE_{PDP}$ are also given in Table 1. The values of $\%IE_{PDP}$ was found to increase with increase in TP extract concentration with the optimal value of 89.8 % obtained for 2.5 g/L inhibitor concentration.

Electrochemical impedance spectroscopy (EIS) studies

Electrochemical impedance spectroscopy studies were also performed to better understand the surface properties of the X80 pipeline steel. The Nyquist plots in the absence and presence of *Thevetia peruviana* (TP) extract are presented in Figure 2. The diagram shows a depressed semicircular capacitive loop which is similar for the different test solutions. This indicates that the corrosion of X80 steel is primarily controlled by charge transfer process at electrode/solution interface and that the mechanism of corrosion is the same for the blank acid solution and the inhibited solutions (Li et al., 2017; Iroha and Hamilton-Amachree, 2019). The diameter of the capacitive loop increased upon the addition of TP extract to 1 M H_2SO_4 solution and is heightened with the increase of the concentration of TP, which confirms that X80 steel corrosion is effectively retarded. However, the capacitive loop are not perfect semi circles, which may be attributed to the inhomogeneity of the steel surface arising from surface roughness or interfacial phenomena (Khaled, 2010) The simple equivalent circuit used to fit the EIS data is embedded in Figure 2, where R_s represents the solution resistance, R_{ct} the charge transfer resistance and CPE is the constant phase element often used in place of double layer capacitance (C_{dl}), as it gives a more precise fitting impedance result. The impedance of CPE (Z_{CPE}) relation is shown in Eq. 5.

$$Z_{CPE} = \frac{(j\omega)^{-n}}{Y_o} \quad (5)$$

Where, Y_0 is the CPE constant, j is the imaginary unit (square root of -1), ω is the angular frequency and n is the phase shift related to surface inhomogeneous (Zheng et al., 2014). The values of C_{dl} are calculated based on Eq. 6. Where, the percentage inhibition efficiency ($\%IE_{EIS}$) was calculated from R_{ct} values using relation shown in Eq. 7.

$$C_{dl} = \left(\sqrt[n]{Y_o}\right)R_{ct}^{\frac{1}{n}-1} \quad (6)$$

$$\%IE_{EIS} = 100\left(1 - \frac{R^{u}_{ct}}{R^{i}_{ct}}\right) \quad (7)$$

Where, R^{u}_{ct} and R^{i}_{ct} are the charge transfer resistance in the absence and presence of TP extract, respectively. The generated EIS parameters are listed in Table 2.

It is clear from Table 2 that the R_{ct} values increases upon addition of TP extract compared to the blank acid solution and an increasing trend is promoted as the concentration of TP extract increases, which could be attributed to the adsorption of TP molecules on the X80 steel surface (Mobin et al., 2016; James and Iroha, 2019). On the other hand, the values of C_{dl} was found to decrease as TP extract concentration increases while inhibition efficiency increased. Decrease in C_{dl} values, could result from a decrease in local dielectric constant and/or the thickness of the electrical double layer, suggesting that the TP molecules function by adsorption at the metal/solution interface (Kumari et al., 2014; El-Hajjaji et al., 2014. The $\%IE_{EIS}$ values increases as TP extract and R_{ct} values increases. The maximum inhibition efficiency for TP extract in 1 M H_2SO_4 reaches up to 94% and these results are in agreement with those obtained from polarisation studies.

Gravimetric measurements

The variation of corrosion rate (CR) and inhibition efficiency (%I_{WL}) with inhibitor concentration at different temperatures are shown in Figures 3 and 4 respectively. It was discovered from the Figures that TP extract inhibits the dissolution of X80 steel in 1 M HCl solution at the various concentrations of the inhibitor studied. This is true because the CR of X80 steel was found to decrease upon addition of TP extract and continued to decrease with increase in the concentration of the extract at the different temperatures studied (Fig. 3). However, the corrosion rate decreased with rise in temperature which strongly suggests that higher temperature increases the energy required for the metal atoms to carry on with dissolution (Obot et al., 2017; Iroha et al., 2015). Figure 4 clearly shows that %I_{WL} increases as inhibitor concentration increases. The maximum %I_{WL} obtained for TP extract is 92.6% at the optimum concentration of 2.5 g/L at 323 K. The explanation to these could be due to the adsorption of inhibitor molecules on the X80 steel surface which hinders the corrosion of the metal in the acid environment.

Surface examination

Table 1: Electrochemical corrosion parameters and inhibition efficiency obtained from PDP curves at 303 K for X80 steel in 1 *M* H_2SO_4 without and with selected TP concentrations

Concentration (g/L)	I_{corr} (mA cm^{-2})	E_{corr} (mV vs SCE)	β_c (mV dec^{-1})	β_a (mV dec^{-1})	IE_{PDP} (%)
Blank	0.995	-456.3	204.8	191.6	
1.5	0.328	-441.3	125.7	118.9	67.0
2.5	0.101	-424.9	104.6	99.1	89.8

Table 2: EIS parameters for X80 steel in 1 *M* H_2SO_4 with and without selected concentrations of TA extract at 30 ^{0}C

Concentration (g/L)	R_s (Ω cm^2)	R_{ct} (Ω cm^2)	n	Y_o (μ $\Omega^{-1}s^2cm^{-2}$)	C_{dl} (μFcm^{-2})	%IE_{EIS} (%)
Blank	0.988	36.2	0.982	245.7	71.62	-
1.5	1.475	120.5	0.889	359.2	27.29	70.0
2.5	1.594	401.8	0.941	149.2	2.96	91.0

Table 3: Calculated thermodynamic parameters from Freundlich adsorption isotherm for X80 pipeline steel corrosion in 1 *M* H_2SO_4 at different temperatures

Temp. (K)	K_{ads} x 10^5	ΔG_{ads}(kJ/mol)	R^2
303	2.49	-41.42	0.9972
313	2.54	-42.84	0.9981
323	2.62	-44.29	0.9960

Table 4: Activation thermodynamic parameters for X80 pipeline steel in 1 *M* H_2SO_4 in the absence and presence of different concentrations of *Thevetia peruviana* extract

Conc. (g/L)	E_a (kJ/mol)	ΔH^*(kJ/mol)	ΔS^* (J/mol/K)
Blank	48.99	34.54	-135.28
0.5	45.72	31.29	-163.95
1.0	43.44	29.01	-169.33
1.5	41.23	27.93	-177.32
2.0	39.32	26.21	-189.29
2.5	38.20	24.97	-193.43

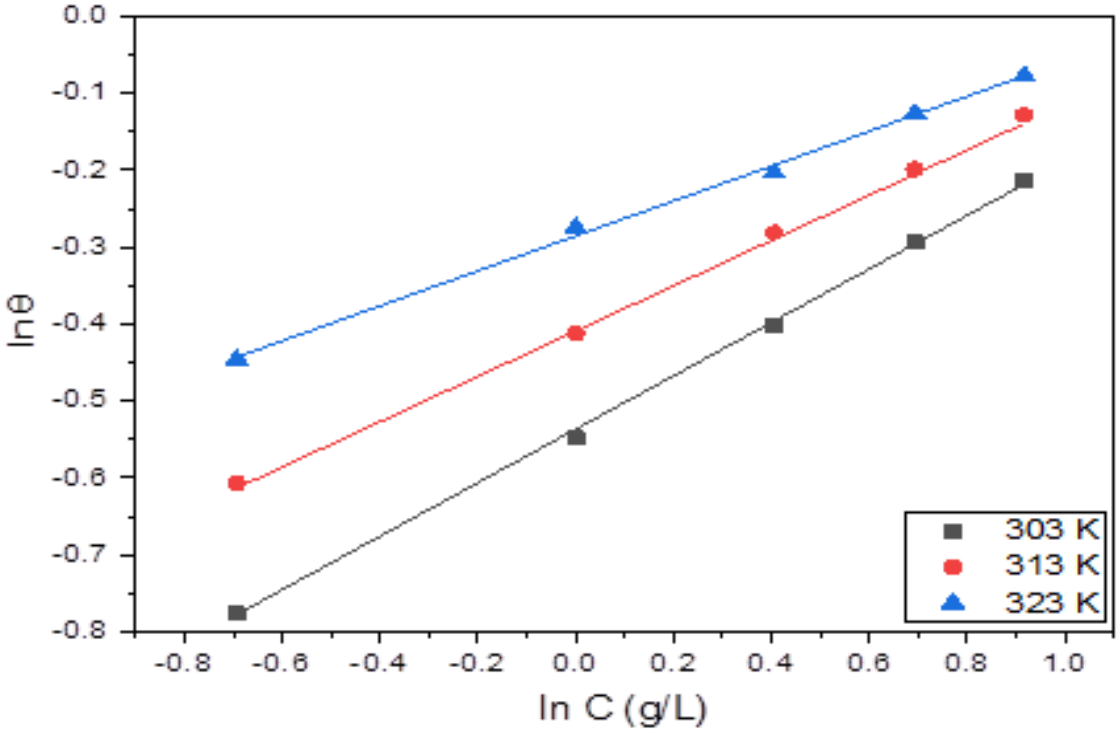

Fig. 6: Freundlich adsorption isotherm of *Thevetia peruviana* extract on X80 steel surface in 1 *M* H_2SO_4 solution at different temperatures

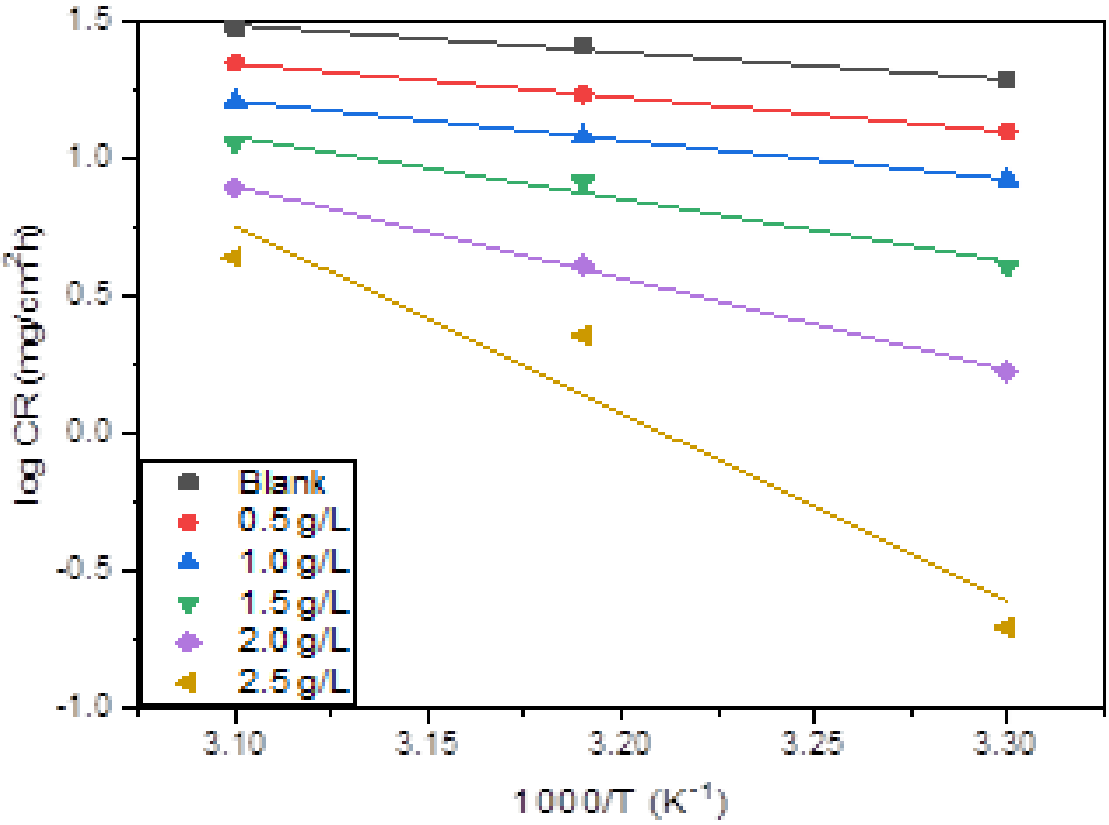

Fig. 7: Arrhenius plots for X80 steel in 1 *M* H_2SO_4 without and with various concentrations of *Thevetia peruviana* extract

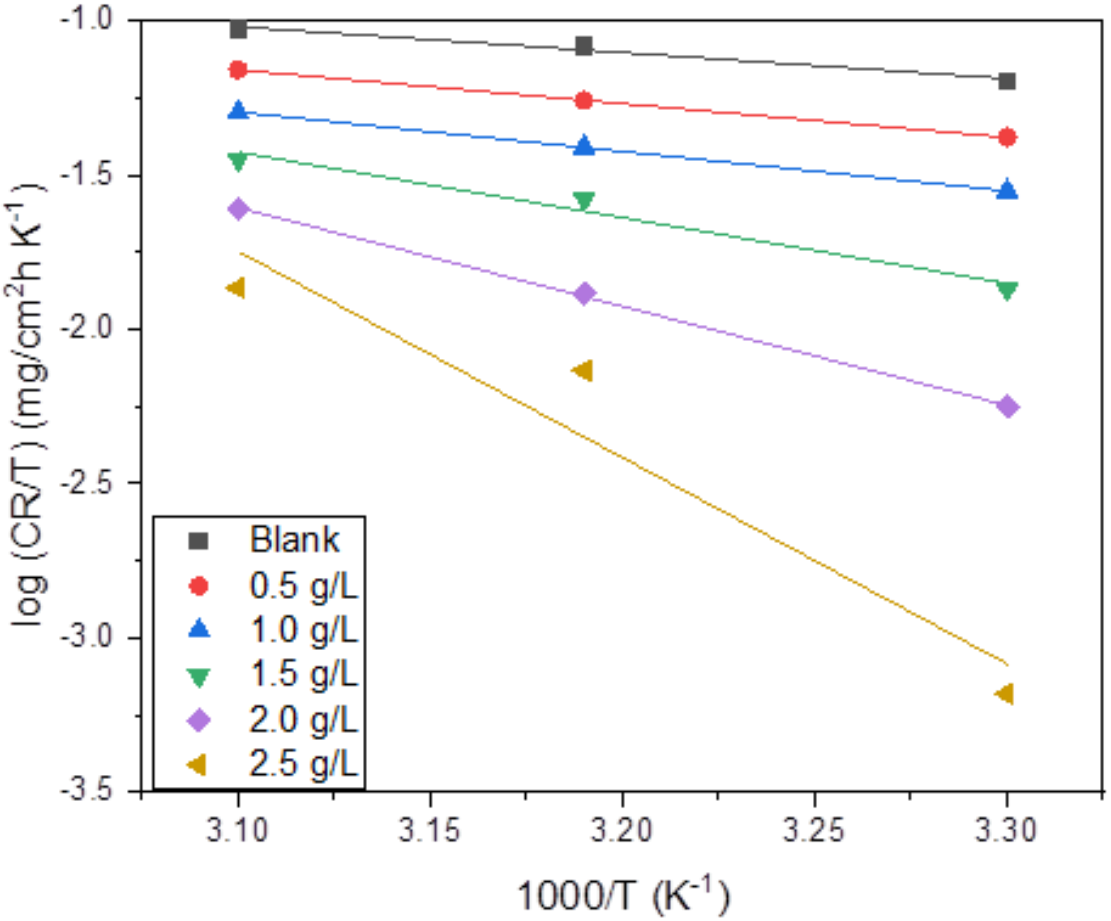

Fig. 8: Transition state plots for X80 pipeline steel in 1 *M* H_2SO_4 in the absence and presence of different concentrations of *Thevetia peruviana* extract.

Surface examination of X80 pipeline steel coupons was made using Scanning electron microscope (SEM) at 30 ◦C. The SEM micrographs of the X80 steel immersed in 1 M H_2SO_4 in the absence and presence of optimum concentration of TP extract are shown in Figures 5a and 5b respectively. From the SEM images, it is seen that the surface of the metal immersed in the solution without the inhibitor is rough as a result of the aggressive corrosion in 1 M H_2SO_4 solution (Figure 5a). On the other hand, smoother surface is observed for the X80 pipeline steel immersed in 1 M H_2SO_4 solution containing TP extract. The smoother surface of the sample in Figure 5b is attributed to the presence of adsorbed protective film on the surface of the X80 pipeline steel which was absent in Figure 5a sample.

Adsorption isotherm

The decrease in corrosion rate of X80 steel is suggestive of the adsorption of *Thevetia peruviana* (TP) extract onto the surface of the steel. If this is the case, very crucial information on the interaction between the metal surface and TP extract can be provided by the use of adsorption isotherms (Ansari et al., 2015). The results obtained from gravimetric measurement were used to plot several adsorption isotherms and it is ascertained that the process seems to follow the Freundlich adsorption isotherm based on the correlation coefficient (R^2) value. Freundlich isotherm is expressed by the following Eq. 8.

$$\ln \theta = \ln K_{ads} + n \ln C \quad (8)$$

Where, θ is the degree of surface coverage, K_{ads} is the adsorption equilibrium constant, *n* is the interaction parameter and C is the inhibitor concentration. The plot of ln θ against ln C at different temperatures is given in Figure 6. The adsorption parameters obtained from Freundlich adsorption isotherm are listed in Table 3. The R^2 values as seen in Table 3 are close to unity which indicates that the adsorption of TP extract molecules onto the X80 steel surface obeys Freundlich isotherm. The values K_{ads} are seen to increase with temperature rise suggesting that TP extract molecules may be chemically adsorbed onto the X80

steel surface. The adsorption equilibrium constant, K_{ads} is related to Gibbs free energy of adsorption, ΔG_{ads} as shown in Eq. 9 (Madueke and Iroha, 2018):

$$\Delta G_{ads} = -2.303RT \log(55.5K_{ads}) \quad (9)$$

Where, 55.5 is the concentration of water, R is the universal gas constant and T is the absolute temperature. The calculated values of ΔG_{ads} presented in Table 3 are all negative suggesting that the adsorption rates were spontaneous and the interaction between the inhibitive molecules was found to be repulsive. These values are in the range -41.42 and -44.29 kJ mol^{-1} which supports the possibility of chemical adsorption mechanism (Ammal et al., 2018; Iroha and James, 2018).

Effect of temperature

As previously observed, the rate of X80 steel corrosion in 1 M H_2SO_4 solution containing different concentrations of *Thevetia peruviana* (TP) leaves extract increases as temperature increases (Fig. 3). In the same manner, inhibition efficiency of the extract increases with increase in temperature (Fig. 4). Increase in inhibition efficiency with temperature rise is often attributed to chemical adsorption of the inhibitor molecules on the metal surface. The relationship between the rate of corrosion and temperature can be better understood using the Arrhenius equation presented in Eq. 10 (Iroha and James, 2019; Solomon et al., 2017):

$$\log CR = \log A - \frac{E_a}{2.303RT} \quad (10)$$

Where, CR is the corrosion rate, A is the Arrhenius constant (pre-exponential factor), R is the universal gas constant, and T is the absolute temperature. Arrhenius plots of log CR versus 1/T depicted in Figure 7 gives a linear curve with slope of $-E_a/2.303R$ from which E_a values were evaluated listed in Table 4.

The values E_a for X80 steel corrosion in the presence of TP extract are in the range of 35.20 KJ/mol to 48.99 KJ/mol but less than the threshold value required in confirming chemical adsorption, suggesting that the adsorption of TP leaves extract on the surface of the steel may have been a combination of physical and chemical adsorption mechanism. The enthalpy, Δ H* and entropy, Δ S* of activation for the adsorption process were obtained based on the transition state Eq. 11.

$$\log\left(\frac{CR}{T}\right) = \left[\left(\log\left(\frac{R}{Nh}\right) + \left(\frac{\Delta S^*}{2.303R}\right)\right)\right] - \frac{\Delta H^*}{2.303RT} \quad (11)$$

Where, h is the Planck's constant and N is the Avogadro's number. The plot of log (CR/T) against 1/T shown in Figure 7 gave a straight line with a slope = (-ΔH*/2.303R) and an intercept = log [(R/Nh)-(ΔS*/2.303R)], from which ΔH* and ΔS* values respectively were obtained and also listed in Table 4. The values of ΔS* in the absence and presence of TP extract are negative, suggesting that the activation stage of the adsorption process represents associative interactions between the steel and the inhibitor molecules rather than dissociative formation of iron and water molecules (Mourya et al., 2015). The positive values of ΔH* reflects the endothermic nature of the X80 steel dissolution process. These findings revealed that the *T. peruviana* extracts are highly efficiency for the inhibition of corrosion and could be potential for inhibition of steel corrosion in acidic environment, which is a problematic issue (Alamri and Obot, 2019; Ayukayeva et al., 2019; Bhuvaneshwari et al., 2019; Chauhan et al., 2019; Obot et al., 2019; Pakiet et al., 2019; Qian and Cheng, 2019; Zhang et al., 2019).

CONCLUSIONS

The extract from *Thevetia peruviana* (TP) leaves was tested for its corrosion inhibition performances on X80 pipeline steel in 1 M H_2SO_4 solution using gravimetric and electrochemical techniques, including SEM analyses. From the results of the study, TP showed appreciable corrosion inhibition performances for X80 steel in the acid solution. The inhibition efficiency increases with increasing concentration of the extract and temperature. The adsorption behaviour of the studied inhibitor obeys Freundlich adsorption isotherm and involves both physical and chemical adsorption mechanisms with predominance of chemisorption. Gravimetric and electrochemical impedance spectroscopy measurements affirm that the inhibitive ability of the inhibitor depends on adsorption of its molecules on the X80 steel surface. Potentiodynamic polarization reveals that TP extract behaves as a mixed-type inhibitor. SEM micrographs confirm the formation of a protective film on the X80 steel surface.

REFERENCES

Ammal, P.R., Prajila, M., Joseph, A., 2018. Effective inhibition of mild steel corrosion in hydrochloric acid using EBIMOT, a 1, 3, 4-oxadiazole derivative bearing a 2-ethylbenzimidazole moiety: electro analytical, computational and kinetic studies. Egyptian Journal of Petroleum 27, 823–833.

Ansari, K.R., Quraishi, M.A., Singh, A., 2015. Isatin derivatives as a non-toxic corrosion inhibitor for mild steel in 20% H_2SO_4. Corrosion Science 95, 62-70.

El-Hajjaji, F., Zerga, B., Sfaira, M., Taleb, M., Ebn Touhami, M., Hammouti, B., Al-Deyab, S.S., Benzeid, H., Essassi, E.M., 2014; Comparative Study of Novel N-Substituted

Quinoxaline Derivatives towards Mild Steel Corrosion Hydrochloric Acid: Part 1. Journal of Materials and Environmental Science, 5(1), 255-262.

Ekanem, U.F., Umoren, S.A., Udousoro, I.I., Udoh, A.P., 2010. Inhibition of mild steel corrosion in HCl using pineapple leaves (*Ananas comosus L.*) extract. Journal of Materials Science, 45, 5558–5566

Iroha, N.B., Akaranta, O., James, A.O., 2012a. Corrosion Inhibition of Mild Steel in Acid Media by Red Peanut skin extract-furfural Resin, Advances in Applied Science Research, 3(6), 3593-3598.

Iroha N.B., Akaranta O., James A.O., 2012b. Red onion skin extract-furfural resin as corrosion inhibitor for aluminium in acid medium. Der Chemica Sinica, 3(4), 995-1001.

Iroha, N.B., Akaranta, O., James, A.O., 2015. Red onion skin extract-formaldehyde resin as corrosion inhibitor for mild steel in hydrochloric acid solution. International Research Journal of Pure & Applied Chemistry, 6(4), 174-181.

Iroha, N.B., Chidiebere, M.A., 2017. Evaluation of the Inhibitive Effect of *Annona Muricata .L* Leaves Extract on Low-Carbon Steel Corrosion in Acidic Media. International Journal of Materials and Chemistry 7(3), 47-54.

Iroha, N.B., Hamilton-Amachree, A., 2019. Inhibition and adsorption of oil extract of *Balanites aegyptiaca* seeds on the corrosion of mild steel in hydrochloric acid environment, *World Scientific News,* 126, 183-197.

Iroha N.B., James A.O., 2019. Adsorption behavior of pharmaceutically active dexketoprofen as sustainable corrosion Inhibitor for API X80 carbon steel in acidic medium. World News of Natural Sciences, 27, 22-37.

Iroha, N.B., James, A.O., 2018. Assessment of performance of velvet tamarind-furfural resin as corrosion inhibitor for mild steel in acidic solution. Journal of Chemical Society of Nigeria, 43(3), 510–517.

Iroha, N.B., Nnanna, L.A., 2019. Electrochemical and Adsorption Study of the anticorrosion behavior of Cefepime on Pipeline steel surface in acidic Solution, Journal of Materials and Environmental Sciences, 10(10), 898-908.

James, A.O., Iroha, N.B., 2019. An Investigation on the Inhibitory Action of Modified Almond Extract on the Corrosion of Q235 Mild Steel in Acid Environment, IOSR Journal of Applied Chemistry, 12(2), 01-10.

Keles, H., Keles, M., Dehri, I., Serindag, O., 2008. The inhibitive effect of 6-amino-m-cresol and its Schiff base on the corrosion of mild steel in 0.5M HCl medium. Materials Chemistry and Physics, 112, 173-179.

Khaled, K.F., 2010. Studies of iron corrosion inhibition using chemical, electrochemical and computer simulation techniques. Electrochimica Acta 55 (22), 6523–6532.

Kumari P.P., Rao S.A., Shetty P., 2014. Corrosion Inhibition of Mild Steel in 2 M HCl by a Schiff Base Derivative. Procedia Materials Science, 5, 499-507.

Li, X., Deng, S., Lin, T., Xie, X., Du, G., 2017). 2-Mercaptopyrimidine as an effective inhibitor for the corrosion of cold rolled steel in HNO3 solution. Corrosion Science 118, 202.

Loto C.A., Loto R.T., Popoola A.P.I., 2011. Effect of neem leaf (*Azadirachita indica*) extract on the corrosion inhibition of mild steel in dilute acids, International Journal of the Physical Sciences, 6(9), 2249-2257.

Madueke, N.A., Iroha, N.B., 2018, Protecting aluminium alloy of type AA8011 from acid corrosion using extract from Allamanda cathartica leaves, International Journal of Innovative Research in Science, Engineering and Technology, 7(10), 10251-10258.

Mobin, M., Zehra, S., Aslam, R., 2016. l-Phenylalanine methyl ester hydrochloride as a green corrosion inhibitor for mild steel in hydrochloric acid solution and the effect of surfactant additive. RSC Advances 6(7), 5890-5902.

Mourya, P., Singh, P., Tewari, A.K., Rastogi, R.B., Singh, M.M. 2015. Relationship between structure and inhibition behaviour of quinolinium salts for mild steel corrosion: Experimental and theoretical approach. Corrosion Science 95, 71–87

Nnanna, L., Onwuagba, B., Mejeha, I., Okeoma, K., 2010. Inhibition effect of Some Plant Extracts on the Acid Corrosion of Aluminium Alloy. African Journal of Pure and Applied Chemistry 4(1), 011-016.

Nwosu, O.F., Nnanna, L.A., Osarolube, E., 2013. The Use of Eco-Friendly Leaf as a Corrosion Inhibitor of Mild Steel in an Acidic Environment. International Journal of Materials and Chemistry 3(3), 64-68.

Obot, I.B., Onyeachu, I.B., Kumar, A.M., 2017. Sodium alginate: A promising biopolymer for corrosion protection of API X60 high strength carbon steel in saline medium. Carbohydrate Polymers, 178, 200–208.

Samal, K.K., Sahu, H.K. Gopalakrishnakone, P. 1992. Clinico-pathological study of *Thevetia peruviana* (yellow oleander) poisoning. Journal of Wilderness Medicine, 3(4), 382-386.

Solmaz, R., 2010. Investigation of the inhibition effect of 5-((E)-4-phenylbuta-1,3-dienylideneamino)-1,3,4-thiadiazole-2-thiol Schiff base on mild steel corrosion in HCl acid. Corrosion Science, 52(10), 3321–3330.

Solomon, M.M., Gerengi, H., Kaya, T., Kaya, E., Umoren, S.A., 2017. Synergistic inhibition of St37 steel corrosion in

15% H2SO4 solution by chitosan and iodide ion additives. Cellulose 24, 931–950.

Soltani, N., Khayatkashani, M., 2015. *Gundelia tournefortii* as a green corrosion inhibitor for mild steel in HCl and H_2SO_4 solutions. International Journal of Electrochemical Science, 10(1), 46–62.

Wang, X., Yang, H., Wang, F., 2011. An investigation of benzimidazole derivative as corrosion inhibitor for mild steel in different concentration HCl solutions. Corrosion Science, 53, 113-121.

Wang, Y., Zhao, W., Ai, H., Zhou, X., Zhang, T., 2011, Effects of strain on the corrosion behaviour of X80 steel. Corrosion Science, 53(9), 2761-2766.

Zhao, W., Xin, R., He, Z., Wang, Y., 2012. Contribution of anodic dissolution to the corrosion fatigue crack propagation of X80 steel in 3.5 wt.% NaCl solution. Corrosion Science 63, 387-392.

Zheng, X., Zhang, S., Li, W., Yin, L., He, J., Wu, J., 2014. Investigation of 1-butyl-3-methyl-1H-benzimidazolium iodide as inhibitor for mild steel in sulfuric acid solution. Corrosion Science 80, 383.

Pradipta, I., Kong, D., Tan, J.B.L., 2019. Natural organic antioxidants from green tea inhibit corrosion of steel reinforcing bars embedded in mortar. Construction and Building Materials 227, 117058.

Qasim, A., Khan, M.S., Lal, B., Shariff, A.M., 2019. A perspective on dual purpose gas hydrate and corrosion inhibitors for flow assurance. Journal of Petroleum Science and Engineering 183, 106418.

Tang, Z., 2019. A review of corrosion inhibitors for rust preventative fluids. Current Opinion in Solid State and Materials Science 23, 100759.

Belwal, T., Ezzat, S.M., Rastrelli, L., Bhatt, I.D., Daglia, M., Baldi, A., Devkota, H.P., Orhan, I.E., Patra, J.K., Das, G., Anandharamakrishnan, C., Gomez-Gomez, L., Nabavi, S.F., Nabavi, S.M., Atanasov, A.G., 2018. A critical analysis of extraction techniques used for botanicals: Trends, priorities, industrial uses and optimization strategies. TrAC Trends in Analytical Chemistry 100, 82-102.

Thakur, M., Bhattacharya, S., Khosla, P.K., Puri, S., 2019. Improving production of plant secondary metabolites through biotic and abiotic elicitation. Journal of Applied Research on Medicinal and Aromatic Plants 12, 1-12.

Alamri, A.H., Obot, I.B., 2019. Highly efficient corrosion inhibitor for C1020 carbon steel during acid cleaning in multistage flash (MSF) desalination plant. Desalination 470, 114100.

Ayukayeva, V.N., Boiko, G.I., Lyubchenko, N.P., Sarmurzina, R.G., Mukhamedova, R.F., Karabalin, U.S., Dergunov, S.A., 2019. Polyoxyethylene sorbitan trioleate surfactant as an effective corrosion inhibitor for carbon steel protection. Colloids and Surfaces A: Physicochemical and Engineering Aspects 579, 123636.

Bhuvaneshwari, B., Vivekananthan, S., Sathiyan, G., Palani, G.S., Iyer, N.R., Rai, P.K., Mondal, K., Gupta, R.K., 2019. Doping engineering of V-TiO2 for its use as corrosion inhibitor. Journal of Alloys and Compounds, 152545.

Chauhan, D.S., Madhan Kumar, A., Quraishi, M.A., 2019. Hexamethylenediamine functionalized glucose as a new and environmentally benign corrosion inhibitor for copper. Chemical Engineering Research and Design 150, 99-115.

Obot, I.B., Solomon, M.M., Umoren, S.A., Suleiman, R., Elanany, M., Alanazi, N.M., Sorour, A.A., 2019. Progress in the development of sour corrosion inhibitors: Past, present, and future perspectives. Journal of Industrial and Engineering Chemistry 79, 1-18.

Pakiet, M., Tedim, J., Kowalczyk, I., Brycki, B., 2019. Functionalised novel gemini surfactants as corrosion inhibitors for mild steel in 50 mM NaCl: Experimental and theoretical insights. Colloids and Surfaces A: Physicochemical and Engineering Aspects 580, 123699.

Qian, S., Cheng, Y.F., 2019. Synergism of imidazoline and sodium dodecylbenzenesulphonate inhibitors on corrosion inhibition of X52 carbon steel in CO2-saturated chloride solutions. Journal of molecular liquids 294, 111674.

Zhang, T., Jiang, W., Wang, H., Zhang, S., 2019. Synthesis and localized inhibition behaviour of new triazine-methionine corrosion inhibitor in 1 M HCl for 2024-T3 aluminium alloy. Materials Chemistry and Physics 237, 121866.